



25th ABCM International Congress of Mechanical Engineering
October 20-25, 2019, Uberlândia, MG, Brazil

COBEM-2019-XXXX

PIV MEASUREMENT OF THE NON REACTING FLOW FIELD IN A FLAMELESS COMBUSTION CHAMBER

Helio Henrique Santomo Villanueva

Guenther Carlos Krieger Filho

Department of Mechanical Engineering, Polytechnic School of University of Sao Paulo, Sao Paulo, 05508-030, Brazil

heliovillanueva@usp.br, guenther@usp.br

Abstract. *This paper presents the first approach at studying the flow field in a flameless combustion chamber using PIV. A non-reactive flow test case from literature was chosen for validation of the experimental test bench and measurement technique. Two components of the averaged velocity field in an area of 100x62 mm² with a resolution of 0.6 mm was acquired by a 12-bit Phantom camera at 1.4 kHz for 2.38 s. Solid seeding particles of Silicon dioxide SiO₂ were used with a 527 nm high-repetition laser. Important characteristics of the flow field in the flameless combustion chamber as the recirculation zone and velocity magnitudes were observed. The result obtained using PIV shows good agreement with a CFD simulation. Results are sensible to the cylindrical optical access and specific image processing techniques were applied.*

Keywords: *MILD combustion, Flameless oxidation, Particle Image Velocimetry*

1. INTRODUCTION

Flameless combustion has been the subject of research in recent years for its lower pollutant emission as NO_x , CO and noise compared to conventional flame regime (Perpignan *et al.*, 2018; Cheong *et al.*, 2017; Khidr *et al.*, 2017; King *et al.*, 2017). It was noticed that the reactants temperature must be greater than the mixture autoignition temperature to achieve the flameless regime (Wunning and Wunning, 1997) and one proposed way is by recirculating the hot combustion products to mix with the fresh reactants (Cavaliere and de Joannon, 2004).

A Flameless combustion chamber using internal recirculation was developed for a wide range of operating conditions (Rebola *et al.*, 2013). The influence of the thermal input (Veríssimo *et al.*, 2013a) and inlet air velocity (Veríssimo *et al.*, 2013b) on the pollutant emission, temperature field, and major species were assessed experimentally. These studies concluded that in flameless regime, the peaks in temperature are attenuated and the temperature distribution is more uniform in comparison to the conventional flame regime.

Integral characteristics of the non reacting flow field of a flameless combustion chamber were assessed using Laser Doppler Anemometry (LDA). Veríssimo *et al.* (2013b) presented the in-plane averaged velocities in 100 points for three cases with different air inlet velocity. As expected the magnitude of the velocity field changes in each case but, it was observed that the recirculation zone position and size do not alter by changing the air inlet velocity.

Although some operational parameters and integral characteristics were already studied, the onset transition from conventional flame to flameless regime and its fundamentals are still questions under research. Direct Numerical Simulations (DNS) of premixed (Minamoto and Swaminathan, 2015), non-premixed (Göktolga *et al.*, 2015) and experimental Planar Laser Induced Fluorescence (PLIF) (Zhou *et al.*, 2017) indicate that at the flame thickness scale, the reaction still occurs in thin zones that are strongly wrinkled by turbulence in such a way that it self-interacts. This effect of turbulence combined with the dilution of the reactants with the burnt gases, results in a less intense reaction rate but present in a greater region compared with the conventional flame.

Zhou *et al.* (2017) also concluded that what makes the flame not visible is the emission reduction of the CH intermediate specie in the reaction zone. Although there are thin reaction zones, their less intense reaction rates results in smaller temperatures. Hence, NO_x production is reduced since the thermal NO formation mechanism is suppressed.

The purpose of this work is the validation of the Particle Image Velocimetry (PIV) technique applied to a flameless combustion chamber assessing its non reacting flow case as a first step at the experimental study of the influence of turbulence on the flameless combustion regime.

2. METHODOLOGY

The flameless combustion chamber manufactured was based on the design of Veríssimo *et al.* (2011) and is illustrated in figure 1a. The cylindrical chamber has a quartz tube of 100 mm diameter and 350 mm long which enable optical access throughout the combustion chamber volume. A non-premixed configuration is adopted for the reactants inlets. Air enters the chamber at the symmetry axis in a 10 mm diameter nozzle and methane in 16 nozzles of 2 mm diameter positioned radially with 15 mm from the symmetry axis. Compressed air system was used for air supply with a nominal mass flow of 3.84×10^{-3} kg/s at atmospheric conditions and 2.04×10^{-4} kg/s of methane as fuel supply. Silicium dioxide SiO_2 particles of 0.23 g/cm^3 and $0.3 \mu\text{m}$ mean diameter were used with the 10F01 powder seeding generator from Dantec Dynamics. Only the air flow was seeded since it is one order of magnitude higher in mass flow.

The laser, a frequency-doubled dual-cavity Nd:YLF Litron Lasers LDY302 527 nm is placed perpendicularly to the high-speed CMOS camera (v311 - Vision Research Inc.) configuring a planar two-component PIV system (2D2C). The laser is equipped with a set of cylindrical lens which creates a sheet with thickness of the order of 1 mm .

The 12-bit camera is equipped with a sensor array of 1280×800 pixels and $20 \mu\text{m}$ of pixel pitch. The set of Carl Zeiss lenses of 50 mm focal length and 1.4 f-number coupled with a 8 mm extension ring are mounted on the high-speed camera. The image acquisition is performed with a $527 \pm 5 \text{ nm}$ bandpass optical filter mounted on the lenses to reduce the interference of ambient light. Laser and camera are synchronized with the pulse delay generator model 575-8C (Berkeley Nucleonics Corporation) and controlled by Dynamic Studio software (Dantec Dynamics A/S) in the acquisition computer. Figure 1b illustrates the PIV test bench and the area of measured velocity components.

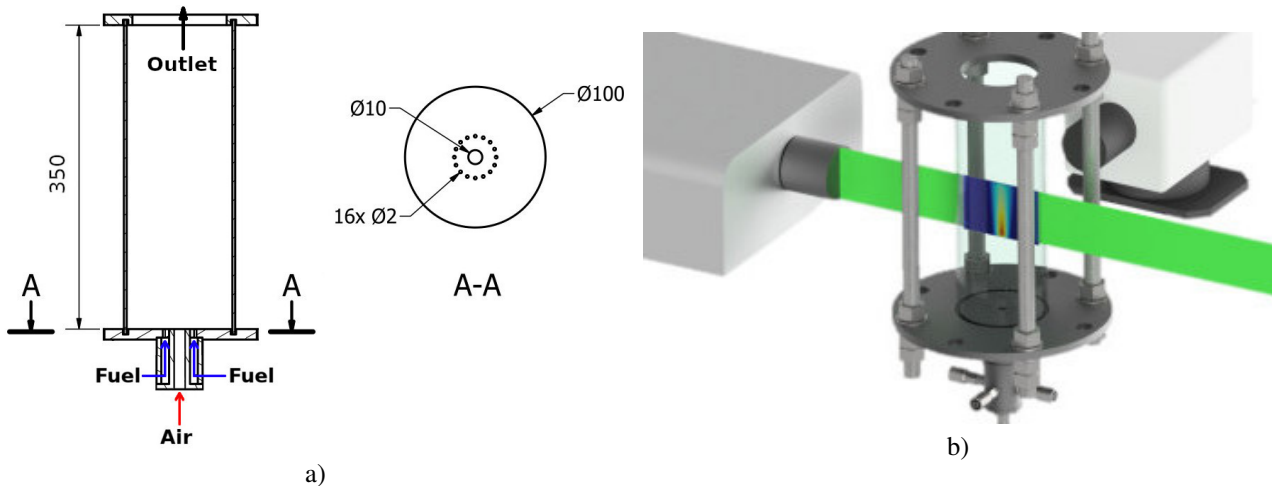


Figure 1. Flameless combustion chamber geometry a) and experimental test bench for PIV measurement b).

Particle images in a Field-of-View (FOV) of $100 \times 62 \text{ mm}^2$, in double-frame mode with $5 \mu\text{s}$ were acquired at 1.4 kHz for 2.38 s resulting in a total of 3,808 image pairs. Vector maps were processed using adaptive PIV algorithm with minimum and maximum interrogation window of 16 and 60 pixels, respectively and 8 pixel step. The resulted vector maps have approximately 0.6 mm resolution with 159×99 vectors in radial and y directions. A pre-processing phase was applied to enhance the cross-correlation estimation. The acquired images were first treated to remove static background by average image subtraction.

3. RESULTS

3.1 Combustion chamber operating in flameless regime

A first validation of the test bench and the combustion chamber was done by operating it under the three different combustion regimes studied by Zhou *et al.* (2017). Conventional flame, transition and flameless combustion. The test conditions for these experiments are given in table 1.

To achieve the flameless regime, the temperature of the reactants must be above the mixture autoignition temperature (Cavaliere and de Joannon, 2004) which may be achieved by mixing the fresh reactants with the combustion products. The idea of this combustion chamber is to dilute the reactants by means of an internal recirculation of the combustion products (Rebola *et al.*, 2013; Veríssimo *et al.*, 2013a,b). Heat transfer through the quartz tube is crucial for this point. A ceramic thermal insulation of 30 mm thick was necessary so to reduce heat loss to the surroundings. It was noticed that temperature close to the cylindrical wall is high enough to make the insulation emits light. Figure 2 shows the combustion chamber under the three regimes. Conventional flame a), transition b) and flameless combustion c).

It was noticed that the combustion behaves differently under the three test conditions. On figure 2a it is possible

Table 1. Test conditions for the three combustion regimes. Conventional, transition and flameless

	Conventional	Air Transition	Flameless	Methane
ϕ	0.53	0.67	0.91	
mass flow [kg/s]	6.59×10^{-3}	5.22×10^{-3}	3.84×10^{-3}	2.04×10^{-4}
Temperature [C]	400	400	400	25

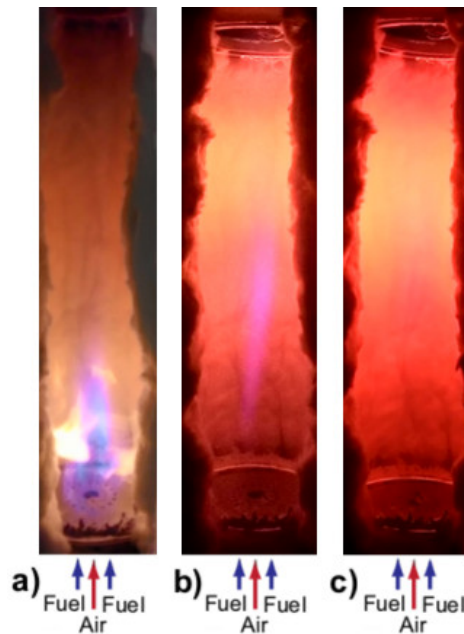


Figure 2. Combustion chamber operating under a) conventional flame, b) transition and c) flameless regimes.

to see light emission from a small region where it is expected to occur the conventional reaction zone. On figure 2b a weak and intermittent light emission was present indicating that the combustion chamber is not operating under a stable conventional flame regime but also not in a flameless regime since the reaction zone still emits visible light. On figure 2c it is not possible to distinguish visually where the chemical reactions are although temperature is still high at the chamber outlet. The temperature at the cylindrical wall is the highest as the thermal insulation emits light brighter in this condition compared to the previous two. It is interesting to note that this light emission occurs close to a uniform distribution which may be due to a uniform temperature distribution throughout the chamber. These characteristics indicate that the combustion chamber is operating under flameless regime and the experimental apparatus were able to reproduce the three combustion regimes as described by Zhou *et al.* (2017).

Another important characteristic to validate the flameless regime is the pollutant emission. It is expected for the flameless case to emit less NO_x and CO than the conventional and transition cases. Evaluation of these species at the outlet of the present chamber will be included for future works.

3.2 PIV results of the non reactive flow

The flameless combustion regime is achieved by pre-heating and diluting the fresh reactants above certain levels related to the reactants mixture. Recirculating the combustion products is one possible alternative for this task as already demonstrated in the literature. For the present combustion chamber, a recirculation structure inside the chamber is expected to occur due to the fluid dynamics. The PIV technique was applied to evaluate this flow characteristic and the analysis were done under the flameless test condition on table 1 without ignition.

Figure 3 shows the time averaged velocity magnitude of the PIV results compared with a CFD simulation using the Reynolds Stress approach for turbulence modelling. It is relevant to note that the distribution of the mean velocity magnitude estimated from the PIV measurement behaves similarly with the calculated CFD result at the measured region. Both results show velocities of one order of magnitude higher close to the axis of symmetry compared to the velocities near the quartz wall with a typical jet stream distribution. Even though a complete mixing of the fuel and air streams is expected at $Y \geq 0.09$ m, the air stream being 18 times higher than the fuel stream indicate that the flow is determined mainly by the air jet.

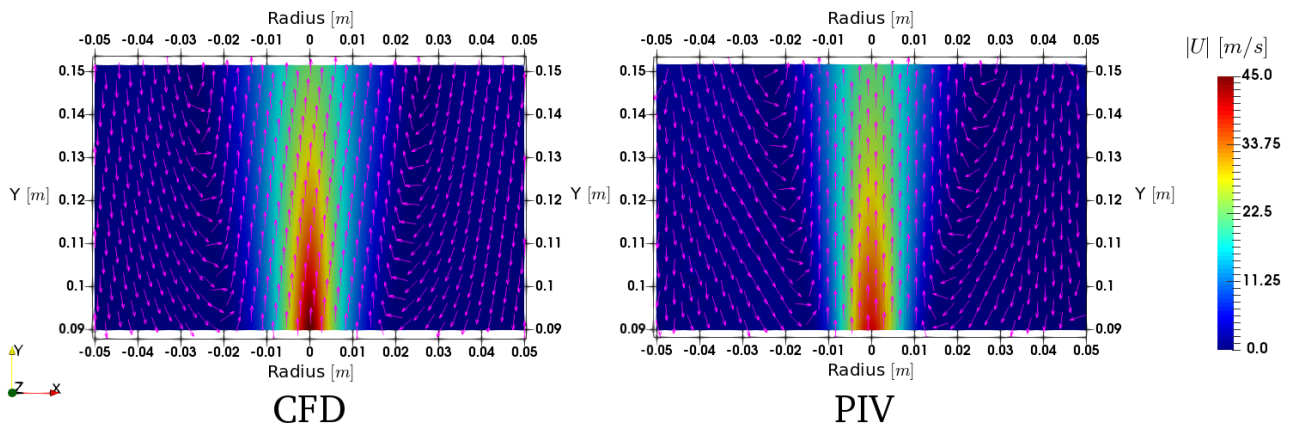


Figure 3. Streamlines calculated from CFD simulation (left) and PIV measurement (right).

The magenta arrows in figure 3 shows that near the central jet, the flow is aligned in the $Y+$ direction but close to the quartz tube the flow is in opposite direction and towards the reactants inlets. An interface with change in flow direction is noticeable, indicating the presence of a recirculation structure in the flow of size in the order of the combustion chamber dimensions. This recirculation will be responsible for directing a fraction of the hot combustion products to mix with the fresh reactants as expected for this combustion chamber design.

Figure 4 shows the mean velocity magnitude profile at the horizontal line of $Y = 0.13$ m calculated from the CFD simulation and estimated from PIV measurements. On both results is clear the symmetric behaviour of the mean velocity profile. Although an overall acceptable agreement between the results, some discrepancies can be seen mainly at the symmetry axis and at the recirculation interfaces. These discrepancies may be caused by the air stream which has an uncertainty of 14% due to the compressed air system available during the current tests.

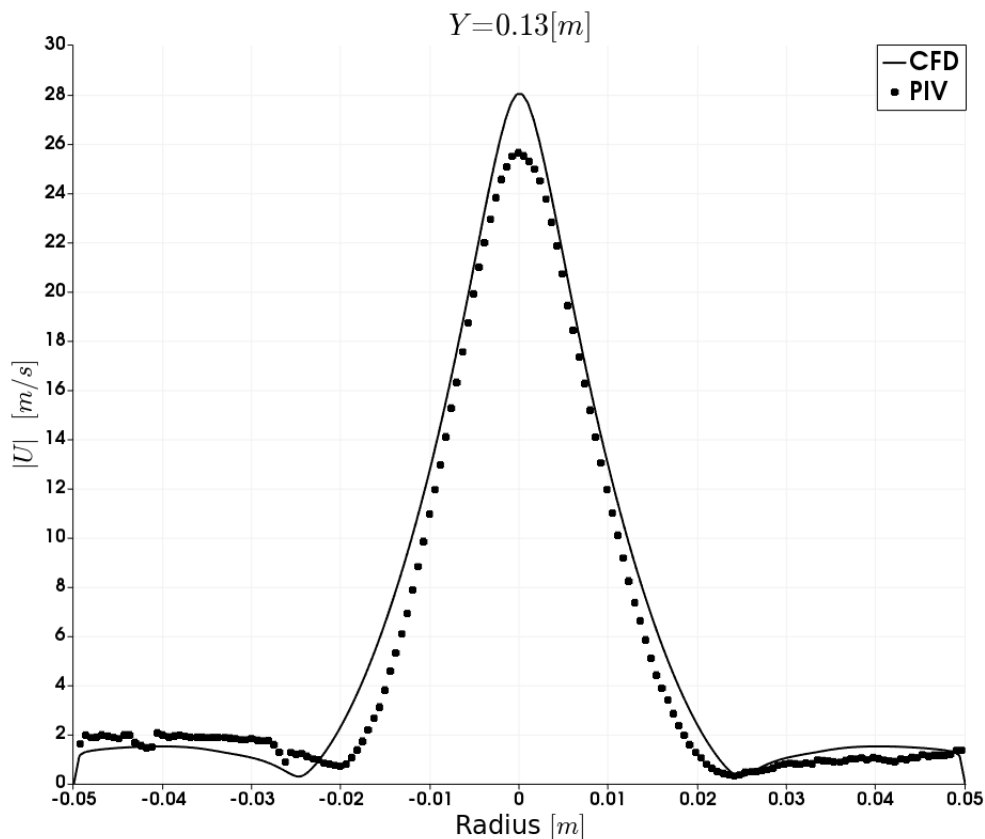


Figure 4. Velocity magnitude profile at horizontal line at $Y = 0.13$ [m].

From the time series and the time averaged velocity distributions, instantaneous velocity fluctuations were estimated allowing the calculation of the Reynolds Stress components $\overline{u_x u_x}$, $\overline{u_y u_y}$, $\overline{u_x u_y}$. Figure 5 shows the Reynolds Stress components at the horizontal line of $Y = 0.13$ m from the CFD and PIV results.

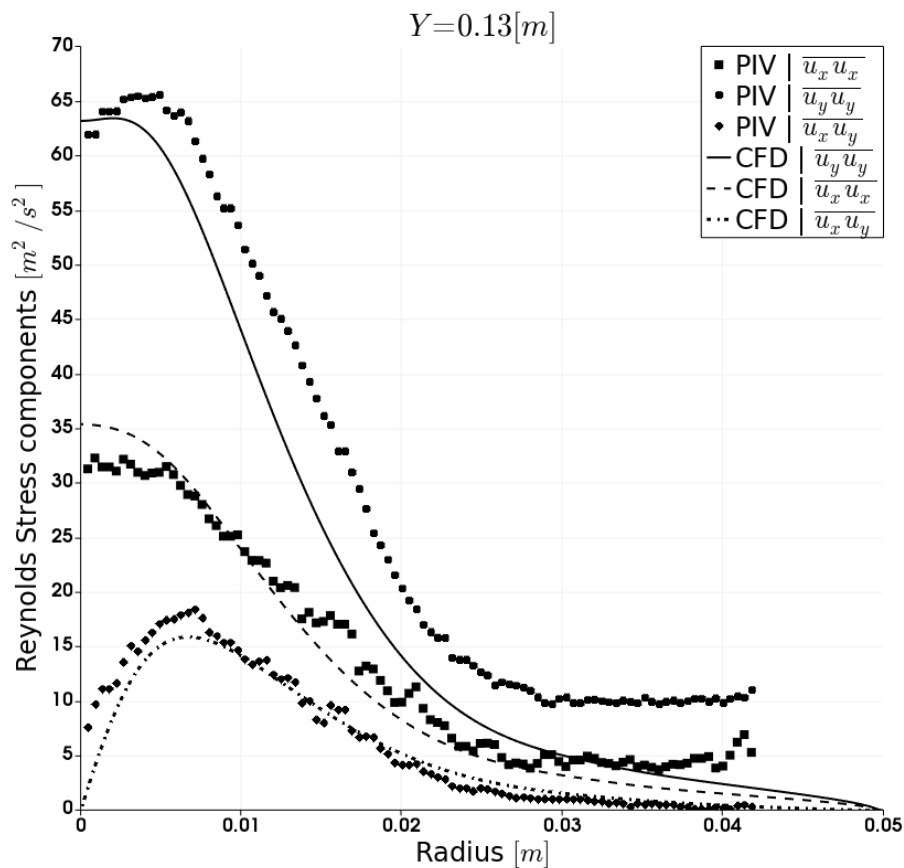


Figure 5. Reynolds Stress components profile at horizontal line at $Y = 0.13$ [m].

The three components behaves similarly for the calculated CFD and estimated PIV results. It is noticeable the directional characteristic of this turbulent flow since the components have different values along the $Y = 0.13$ m line except to very close to the quartz wall where it tends to lower values. The $\overline{u_y u_y}$ component shows the highest values which is aligned with the direction of the central jet flow. The cross component $\overline{u_x u_y}$ has its peak value close to the steeper velocity gradient, which may indicate the position of the highest mixing rate region of the combustion products with fresh reactants, crucial for the flameless combustion process.

4. Conclusions

A flameless combustion chamber was successfully manufactured and operated under three different combustion regimes proposed in literature. The non reactive flow case of the flameless test condition was assessed by the PIV measurement technique in this study. The internal recirculation responsible for directing the hot combustion products to mix with the fresh reactants was observed. The comparison of PIV results with a CFD simulation show good agreement for the mean velocity field within the uncertainty related to the air supply system. The Reynolds Stress components shows the directional characteristic of this turbulent flow in which the component aligned with the central jet has highest values. The cross component indicates the region where mixing of the combustion products and the fresh reactants possibly occur more intensely. Future research is needed for apply this methodology to the reactive flameless case to understand better, not only the differences on the reactive/non-reactive flows with respect on turbulence, but the fundamental parameters, as the production, dissipation and scales of turbulence for the development of the flameless combustion.

5. ACKNOWLEDGEMENTS

The authors would like to acknowledge Escola Politécnica da Universidade de São Paulo, Fundação de Amparo à Pesquisa do Estado de São Paulo (FAPESP) project number FAPESP 2013/50238-3, FAPESP 2014/50279-4 and Conselho Nacional de Desenvolvimento Científico e Tecnológico (CNPq) for the research support.

6. REFERENCES

- Cavaliere, A. and de Joannon, M., 2004. "Mild combustion". *Progress in Energy and Combustion Science*, Vol. 30, No. 4, pp. 329 – 366. ISSN 0360-1285. doi:<http://dx.doi.org/10.1016/j.peccs.2004.02.003>. URL <http://www.sciencedirect.com/science/article/pii/S0360128504000127>.
- Cheong, K.P., Li, P., Wang, F. and Mi, J., 2017. "Emissions of NO and CO from counterflow combustion of CH₄ under MILD and oxyfuel conditions". *Energy*, Vol. 124. ISSN 03605442. doi:10.1016/j.energy.2017.02.083.
- Göktolga, M.U., van Oijen, J.A. and de Goey, L.P.H., 2015. "3D DNS of MILD combustion: A detailed analysis of heat loss effects, preferential diffusion, and flame formation mechanisms". *Fuel*, Vol. 159, pp. 784 – 795. ISSN 0016-2361.
- Khidr, K.I., Eldrainy, Y.A. and EL-Kassaby, M.M., 2017. "Towards lower gas turbine emissions: Flameless distributed combustion". doi:10.1016/j.rser.2016.09.032.
- Minamoto, Y. and Swaminathan, N., 2015. "Subgrid scale modelling for MILD combustion". *Proceedings of the Combustion Institute*, Vol. 35, No. 3, pp. 3529 – 3536. ISSN 1540-7489.
- Perpignan, A.A., Rao, A.G. and Roekaerts, D.J., 2018. "Flameless combustion and its potential towards gas turbines". *Progress in Energy and Combustion Science*, Vol. 69, pp. 28 – 62. ISSN 0360-1285.
- Rebola, A., Costa, M. and Coelho, P.J., 2013. "Experimental evaluation of the performance of a flameless combustor". *Applied Thermal Engineering*, Vol. 50, No. 1, pp. 805–815. ISSN 13594311. doi:10.1016/j.applthermaleng.2012.07.027.
- Veríssimo, A.S., Rocha, A.M.A., Costa, M., Veríssimo, A.S., Rocha, A.M.A. and Costa, M., 2011. "Operational, combustion, and emission characteristics of a small-scale combustor". *Energy and Fuels*, Vol. 25, No. 6, pp. 2469–2480. ISSN 08870624.
- Veríssimo, A.S., Rocha, A.M.A. and Costa, M., 2013a. "Experimental study on the influence of the thermal input on the reaction zone under flameless oxidation conditions". *Fuel Processing Technology*, Vol. 106, pp. 423–428. ISSN 03783820. doi:10.1016/j.fuproc.2012.09.008.
- Veríssimo, A.S., Rocha, A.M.A. and Costa, M., 2013b. "Importance of the inlet air velocity on the establishment of flameless combustion in a laboratory combustor". *Experimental Thermal and Fluid Science*, Vol. 44, pp. 75 – 81. ISSN 0894-1777.
- Veríssimo, A.S., Rocha, A.M.A., Coelho, P.J. and Costa, M., 2015. "Experimental and numerical investigation of the influence of the air preheating temperature on the performance of a small-scale mild combustor". *Combustion Science and Technology*, Vol. 187, No. 11, pp. 1724–1741.
- Wunning, J. and Wunning, J., 1997. "Flameless oxidation to reduce thermal NO-formation". *Progress in Energy and Combustion Science*, Vol. 23, No. 1, pp. 81 – 94. ISSN 0360-1285.
- Xing, F., Kumar, A., Huang, Y., Chan, S., Ruan, C., Gu, S. and Fan, X., 2017. "Flameless combustion with liquid fuel: A review focusing on fundamentals and gas turbine application". *Applied Energy*, Vol. 193, pp. 28–51. ISSN 03062619. doi:10.1016/j.apenergy.2017.02.010.
- Zhou, B., Costa, M., Li, Z., Aldén, M. and Bai, X.S., 2017. "Characterization of the reaction zone structures in a laboratory combustor using optical diagnostics: From flame to flameless combustion". *Proceedings of the Combustion Institute*, Vol. 36, No. 3, pp. 4305–4312. ISSN 15407489. doi:10.1016/j.proci.2016.06.182.

7. RESPONSIBILITY NOTICE

The authors are the only responsible for the printed material included in this paper.